ORIGINAL PAPER

Spatial and temporal variability of water vapor pressure in the arid region of northwest China, during 1961–2011

Junqiang Yao · Yaning Chen · Qing Yang

Abstract This paper investigated the spatial and temporal variations of the water vapor pressure (WVP) of the arid region of northwest China (ARNC) from 1961 to 2011. The original daily temperature and relative humidity data were collected from 96 meteorological stations in the region and analyzed by a Mann–Kendall test and linear trend. The results showed that (1) the WVP possesses vertical zonality and longitude zonality, which decreased from the low to high with the elevation increasing, and the WVP changed obviously from the northwest and southeast to the middle of the ARNC. (2) WVP exhibited an abrupt increasing trend in most of the stations over the past 51 years; only four meteorological stations displayed upward trend in the ARNC. The WVP in the desert increased most rapidly, followed by the oasis and mountainous area. (3) The northwest of Xinjiang and northwest of the Hexi Corridor were sensitive to the water vapor change. Thus, further studies should be performed on the relations between the land use and cover and the water vapor change.

J. Yao · Q. Yang
Institute of Desert Meteorology, Xinjiang Meteorological Adminstration,China Meteorological Administration,
Urumqi 830002, China

J. Yao
College of Resources and Environment, Key Laboratory of Oasis Ecology of Ministry of Education, Xinjiang University,
Urumqi 830046, China

Y. Chen (✉)
State Key Laboratory of Desert and Oasis Ecology, Xinjiang Institute of Ecology and Geography, Chinese Academy of Sciences (CAS),
Urumqi 830011, China
e-mail: chenyn@ms.xjb.ac.cn

1 Introduction

A preponderance of evidence has accumulated over the last half a century showing that the global average temperature is increasing primarily as a result of increased greenhouse gas emissions (IPCC 2007). The water vapor increases exponentially with temperature, and it also contributes to global warming about 60~80%, as the main greenhouse gas responsible for climate change (Held and Soden 2000). Wentz et al. (2007) examined that increased water vapor content (WVC) may increase precipitation. Many researchers have examined water vapor conditions, sources, directions of movement and convergence regarding the formation of heavy rain, and the relations between these factors and the rainy season and rain belts in the East Asian monsoon region, Tibet Plateau, Yangtze River Basin, Yellow River Basin, and other low-latitude regions of China (Huang et al. 1998; Zhou and Yu 2005; Zhao et al. 2008; Li et al. 2012).

The arid region of northwest China, herein referred to as ARNC, holds a strategical important position in China's economic development (Li et al. 2012). Since the late 20th century, the climate changed from warm dry to warm humid in the ARNC and the precipitation increased noticeably due to global warming (Hu et al. 2002; Shi et al. 2007). The water vapor conditions that resulted in these changes have changed markedly. The research of Jin et al. (2006) indicated that the water vapor condition in ARNC was more sensitive to global warming; Wang et al. (2006) analyzed the regional features and variations of water vapor in ARNC based on National Centers for Environmental Prediction (NCEP)/National Center for Atmospheric Research (NCAR) reanalysis data (2.5°×2.5°). Jin et al. and Wei et al. studied the characteristics of variation of water vapor transport (WVT) and precipitation in ARNC (Jin et al. 2006; Wei et al. 2010); Wu et al. (2012) analyzed the possible physical mechanism of WVT over Tarim River Basin. Wang et al. and Yao et al. analyzed the

response of water vapor pressure over the Gansu Province and Tianshan mountains to global climate change (Wang et al. 2006; Yao et al. 2012). Li et al. (2012) studied the spatial and temporal distributions of water vapor in ARNC in summer using the NCEP/NCAR reanalysis data (1° × 1°). However, due to the limitation of available data, there are limited lines of research on the spatial and temporal variability of water vapor pressure and its difference of the mountain, oasis, and desert in ARNC (Wang et al. 2003, 2006).

This study investigates the spatial and temporal variability of water vapor pressure in the mountainous, oasis, and desert areas in ARNC in the past 51 years. These studies will be of importance in revealing the regularity of regional water vapor fluctuations to recognize the evolution of drought and to optimize the utilization of the atmospheric water vapor resources.

2 Study area, data, and methods

2.1 Description of the arid region of northwest China

ARNC is located in the inner most center of the Eurasia continent, ranging from 34 to 50° N and from 73 to 108° E, the vast area between the western Helan Mountain–Zaocys Ridgeline and the northern Kunlun Mountains. The high mountains, such as Tianshan Mountains, Kunlun Mountains, and Qilian Mountains, surrounded the vast desert basins, such as the Tarim Basin and the Junggar Basin. Both arid basins and humid mountains are sensitive to climate change (Shi et al. 2007). In terms of administration, it includes the Xinjiang Uygur Autonomous Region, the Midwest Inner Mongolia Autonomous Region, most part of the Ningxia Hui Autonomous Region, and the Hexi Corridor region in the Gansu Province, which is about 2.5 million square kilometers, accounting for over 25 % of China's total territory. The climate of the arid region is typical of inner continental land masses, due to the long distance to the surrounding oceans, and is dominated by continental arid conditions with

lesser effects from the East Asian Monsoon (Liu et al. 2008). The annual mean temperature is about 8 °C, and annual precipitation is less than 300 mm on mean, gradually decreasing from east to west.

2.2 Data processing

We used the data from the meteorological stations to detect and analyze the WVC variations in ARNC. Ground-based surface vapor pressure (SVP) data were calculated based on observations of 96 meteorological stations in ARNC (Fig. 1). The original daily temperature and relative humidity data were provided by the National Climate Center of China Meteorological Administration (NCC-CMA). All the 96 meteorological stations selected for this study had been maintained following the standard of the National Meteorological Administration of China. The standard requires strict quality control processes including extreme inspection, time consistency check, and others before releasing these data. Daily mean surface temperature and mean relative humidity were utilized to calculate SVP.

Firstly, the saturation vapor pressure was calculated with following equation (Environment Canada 1977):

$$e_s = 0.6107 e^{\left(\frac{17.33T}{239 + T}\right)} \tag{1}$$

where e_s is the saturation vapor pressure (hPa) and T is the surface temperature (°C) (Abbott and Tabony 1985). And then, the saturation vapor pressure and relative humidity were used to calculate the SVP with Eq. (2):

$$e = e_s \times RH \tag{2}$$

where e is the SVP (hPa) and RH is the relative humidity (%). Daily mean SVP data set was generated from January, 1961, to December, 2011.

Chen (2014) found that the areas above 1500 m are the main water supply regions in ARNC. Accordingly, in this study, we used 1500 m as the threshold to define the mountainous areas in ARNC and selected meteorological stations

Fig. 1 The locations of meteorological stations in the arid region of northwest China
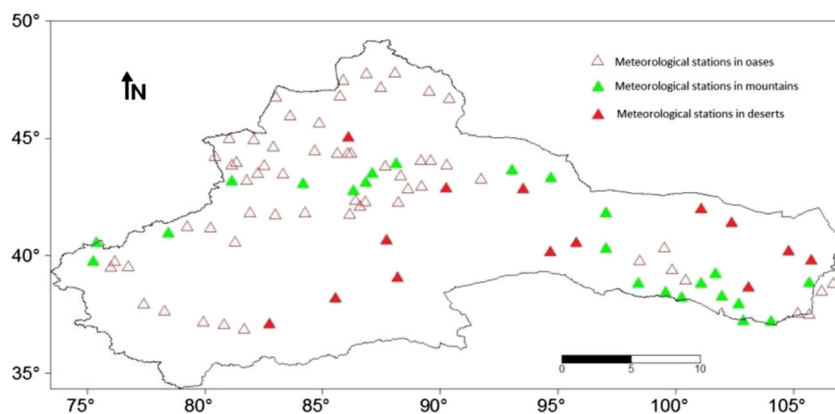
whose altitudes are above this threshold to represent this type of areas. We also considered that the selected stations should be located in areas with few human activities. A total of 23 meteorological stations were selected for the mountainous areas, with a mean altitude of 2185 m. For the oases, we selected those meteorological stations that are located in the large- and medium-sized urban areas with dense populations to reflect the impact of human activities. A total of 59 such meteorological stations were selected, with a mean altitude of 879 m. The number of meteorological stations in the desert areas is very limited. We selected 14 meteorological stations to represent the desert areas. They are either actually located in the desert with fragile ecosystems or in small oases surrounded by deserts and featured by small population, little human activity, and sparse vegetation.

2.3 Methods

2.3.1 Mann–Kendall method for nonparametric test

The nonparametric Mann–Kendall method was used to detect the trends and abrupt change of the climate variability, and originated from Mann (1945) and rephrased by Kendall (1948). The Mann–Kendall method evaluates the trend in the time series of meteorological variables and has been widely used in trend analysis because it does not require the data samples to have a certain distribution (Kahya and Kalayci 2004).

In this method, H_0 represents distribution of random variables and H_1 represents possibility of bidirectional changes. The test statistic S is given by

$$S = \sum_{i=1}^{n-1} \sum_{k=i+1}^{n} \text{sgn}(x_k - x_i) \tag{3}$$

where X_k and X_i are the sequential data values, n is the length of the data set, and

$$\text{sgn}(\theta) = \begin{cases} +1, & \theta > 0 \\ 0, & \theta = 0 \\ -1, & \theta < 0 \end{cases} \tag{4}$$

In particular, if the sample size is larger than ten, the statistic S is nearly normally distributed, i.e., the statistic

$$Z_c = \begin{cases} \dfrac{S-1}{\sqrt{\text{var}(S)}}, & S > 0; \\ 0, & S = 0; \\ \dfrac{S+1}{\sqrt{\text{var}(S)}}, & S < 0; \end{cases} \tag{5}$$

is a standard normal random variable, whose expectation value and variance are as follows:

$$E(S) = 0 \tag{6}$$

$$\text{var}(S) = \left[n(n-1)(2n+5) - \sum_{t} t(t-1)(2t+5) \right]/18 \tag{7}$$

in which t denotes the extent of any given tie and Σ denotes the summation over all ties. In the Mann–Kendall test, another very useful index is the Kendall slope, which is the magnitude of the monotonic trend and is given by

$$\beta = Median\left(\frac{x_i - x_j}{i - j}\right), \forall j < i \tag{8}$$

in which $1 < j < i < n$. A positive value indicates an "upward" trend, i.e., an increase with time, and a negative value indicates a "downward" trend, i.e., a decrease with time.

2.3.2 Mann–Kendall method for abrupt change test

Under the null hypothesis of no trend, the time series of variable has no change and the time series could be regarded as $x_1, x_2 \ldots x_n$. For each term, m_i is computed as the number of later terms in the series whose values exceeded x_i. The test statistic is calculated as follows:

$$d_k = \sum_{i}^{k} (2 \leq k \leq N) \tag{9}$$

Presuming that the series is random and independent, the expected value $E(d_k)$ and variance of d_k could be shown as follows:

$$\begin{cases} E[d_x] = k(k-1)/4 \\ \text{var}[d_k] = \dfrac{k(k-1)(2k+S)}{72} \cdots (2 \leq k \leq N) \end{cases} \tag{10}$$

We define

$$u(d_k) = (d_k - E[d_k])/\sqrt{\text{var}[d_k]} \tag{11}$$

The terms of the $u(d_k)$ $(1 \leq k \leq n)$ constitute curve C_1. The null hypothesis of no trend will be rejected at a confidence level of a if the standard normal probability $\Pr(|u|) < |u(d_k)| > a$. A typical confidence level of 95 % was used with annual total precipitation series. Applying the method to the inverse series, we could obtain the series of $\bar{u}(d_k)$ as follows:

$$\begin{cases} \bar{u}(d_i) = -u(d_i) \cdots (i, i = 1, 2, \cdots n) \\ i = n + 1 - i \end{cases} \tag{12}$$

Fig. 2 The WVP at the meteorological stations in the ARNC for the period 1961–2011
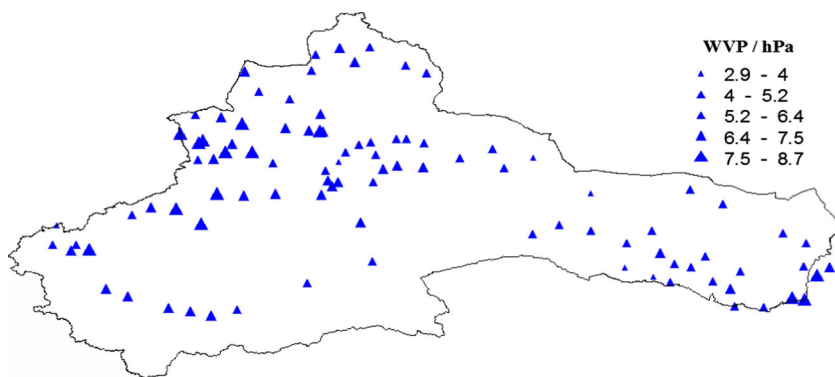
The terms of the $\bar{u}(d_k)$ ($1 \le k \le n$) constitute another curve C_2.

If C_1 exceeds the confidence line, it means that there is a significant upward or downward trend in series. And, if the intersection point of the C_1 and C_2 is between the two confidence lines, we can consider that abrupt climate change took place at that point (Fu and Wang 1992; Liu et al. 2008).

3 Results and analysis

3.1 Spatial patterns of AMWVP

Annual mean water vapor pressure (AMWVP) ranges from 2.9 to 8.7 hPa with high values (5.0–8.7 hPa) from the Ili Valley, the northern and southern slopes of Tianshan Mountainous Area, the northern slope of Kunlun Mountainous Area, and the northwest part of the Ningxia Hui Autonomous Region and with low values (0–5.0 hPa) from the Tianshan Mountainous Area, Qilian Mountainous Area, Altai Mountainous Area, the eastern and southeastern parts of Xinjiang Uygur Autonomous Region, and the Midwest Inner Mongolia Autonomous Region (Fig. 2). The AMWVP high values are found in oasis areas and the low values in mountainous area and desert area. According to Eq. (2), it is clear that the low value in mountains is caused by the low surface temperature which leads to low saturation vapor pressure (e_s), while the low value in desert area results from the low RH. Furthermore, the reasons forming this distribution are due to the different environments, and the variation and complex terrain has led various regional climatic conditions and also led to the spatial differentiation of the AMWVP in ARNC. The fluctuant topography comprised one of the main causes to form the various regional climates in the mountainous area. The oases in the piedmont and intermountainous basin, in addition, occupy less than 5 % of the total area but carry 95 % of the population, and more than 90 % of GDP (Wang 1995) is the most populated and agriculturally developed area, and hence with sufficient moisture, the water vapor pressure (WVP) is high (Li et al. 2012a).

However, it is diverse in desert area. The larger-scale atmospheric circulation, geographical situation, and altitude composed a complex condition to influence the spatial distribution of annual mean water vapor content (AMWVC) in ARNC.

3.2 WVP variations with longitudes and altitude

The relationship between the WVP and longitude, altitude used to reveal the spatial structure of the WVP variation, is shown in Figs. 3 and 4. The results presented that the WVP was linearly negatively related to the altitude, but it was complicated in relation with the longitude. It was suggested that the WVP possesses the vertical zonality; that is, the WVP decreases significantly with altitude. The average altitude in the mountainous area is above 4000 m, and the altitude rises from 100 to 7000 m, but the WVP mainly in lower levels atmospheric (Hu et al. 2002). The correlation between WVP and altitude for higher altitudes is higher than that for low altitudes. The correlation increases in conjunction with the rise of altitude, the highest correlation appears above 2500 m, and the correlation coefficient is 0.95. The cause of lower correlation for low altitudes may be the complex underlying surface, in which the correlation with oasis landscape was higher than
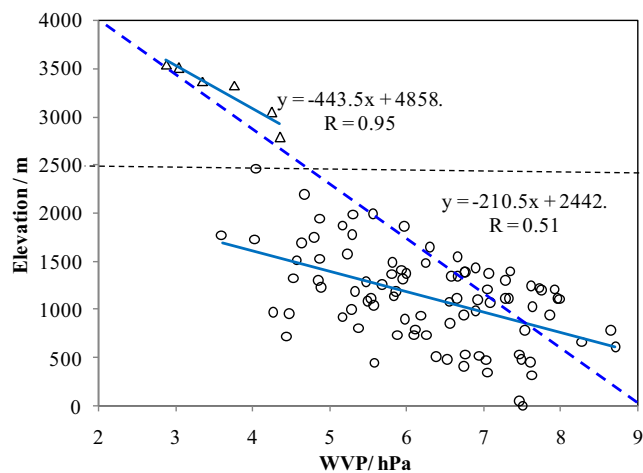

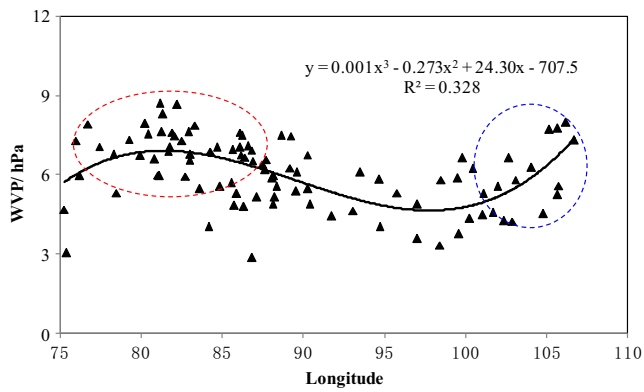**Fig. 3** Relationship between AMWVC and altitude in the ARNC

Fig. 4 Relationship between WVP and longitude in ARNC; the linear fitted model was used to fit the relationship between WVP and longitude, and the linear model and R^2 also are also given in the figure; *the red dashed lines* are the regional of westerly wind, and the *blue dashed lines* are the regional of monsoon

that with desert landscape; the correlation coefficients are 0.59 and 0.24, respectively.

Figure 4 shows the variations of WVP in the ARNC with longitudes. Along longitude from west to east, the WVP displays a variation of "first high value and then low value" with the turning point being at 90° E and exhibits a variation of first low value and then high value with the turning point being at 100° E. The results also indicated that the WVP possesses the longitude zonality, and the WVP changed obviously from the northwest and southeast to the middle of the ARNC. The

northwest portion of the ARNC is subjected to less impact from the East Asian monsoon and the Indian monsoon, and the climate here is most likely caused primarily by the combined effects of the plateau monsoon and the mid-latitude westerly circulation (Sun et al., 2010). Influenced by the plateau monsoon and the westerly circulation, the WVP showed higher value area in this region. The plateau monsoon is formed due to the uplift of the Qinghai–Tibet Plateau and a reverse direction of the winter and summer monsoon, and it caused the moist air from the Indian Ocean and the Bay of Bengal region. The mid-latitude westerly circulation is an additional important circulation that influences the climate change in this area, which brings about abundant warm and wet air from North Atlantic Ocean and Caspian Sea that is likely to sink the atmospheric water vapor and form precipitation when negotiates high mountains (Dai and Wang 2010). The southeast portion of the ARNC is also a higher value area due to its closeness to the sea, influenced by East Asian monsoon and the Indian monsoon. Further, the changes of land use/cover affected by the population explosion and human activities would alter the albedo, evapotranspiration, wind speed, humidity, and radiation to some extent, yielding sensitive negative or positive feedbacks with surface water vapor in the ARNC.

Figure 5 shows that the relationship between WVP and elevation in mountainous area and the vertical profiles of WVP in mountainous area decreases nearly linearly with
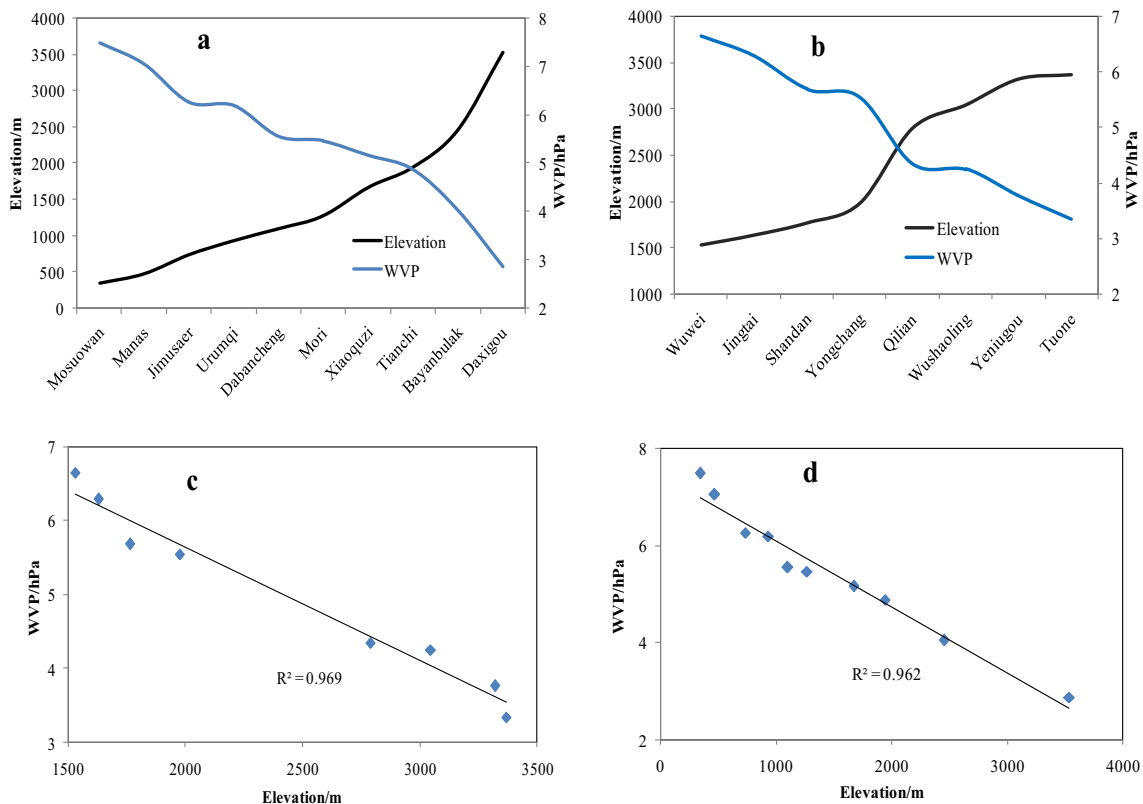

Fig. 5 Relationship between WVP and elevation in Tianshan mountains (**a**, **c**) and Qilian mountains (**b**, **d**)

height (Fig. 4). The value difference of WVP in Qilian mountains and Tianshan mountains of the same elevations is significant because of geological location and environment. More specifically, the WVP of Qilian mountains is greater than that of Tianshan mountains in the same height (Fig. 4c, d). The reasons for these mainly lie in two aspects. Firstly, the East Asian Monsoon, which controlled the climatic situation, affects the WVP in Qilian mountains; these warm humid winds also carry moisture reaching the Qilian mountain from the Pacific and Indian Ocean. However, the fewer westerly winds carry moisture reaching the Tianshan mountains from the Atlantic Ocean through Western Europe and Central Asia. The oasis in the piedmont and intermountainous basin of Qilian mountains, in addition, is the most populated and agriculturally developed area, and hence with sufficient moisture, the WVP is higher.

3.3 Trend analysis of WVP

The Mann–Kendall (M-K) nonparametric statistical test found that the AMWVP in the ARNC has significant increasing trends for the period 1961–2011 ($P<0.01$), with a rate of 0.12 hPa/10a, and indicated abrupt change points in 1986 ($P<0.001$). The rising trend is consistent with the climate change of the entire globe and China (Ren et al. 2005;

Brohan et al. 2006), and the abrupt change points are same for the climate change of the ARNC (Li et al., 2012).

Among the three landscapes, the desert has an increasing rate of 0.15 hPa/10a, the fastest among the three, and it is followed by the oasis with a rate of 0.14 hPa/10a; the mountain has the lowest rate of 0.08 hPa/10a, The M-K test shows that the increasing trends of the three landscapes are statistically significant ($P<0.01$). A possible reason for the mountain landscapes having the slowest increasing rate is the widespread snow and glacier, vegetation diversity, and high ecosystem stability in the mountainous area that have a certain buffer action on the global climate change, while the desert region is vice versa (Li et al., 2012). The WVP rising trend in the three landscapes is consistent with the temperature change of the ARNC, in which the temperature has increased at 0.325, 0.339, and 0.360 °C per decade in the mountainous, oasis, and the desert areas in the recent 50 years, respectively (Li et al., 2012); the reasons forming this consistent change are mainly due to that temperature rising strengthens local circulation and improves water vapor in the air (Li et al. 2012b). Bengtsson (1997) found that the temperature rising leads to increase atmospheric water vapor by 15 %.

The M-K test found that the abrupt change of WVP in the entire areas occurred in 1986 ($P<0.01$), which is consistent with the findings of previous research for the temperature and
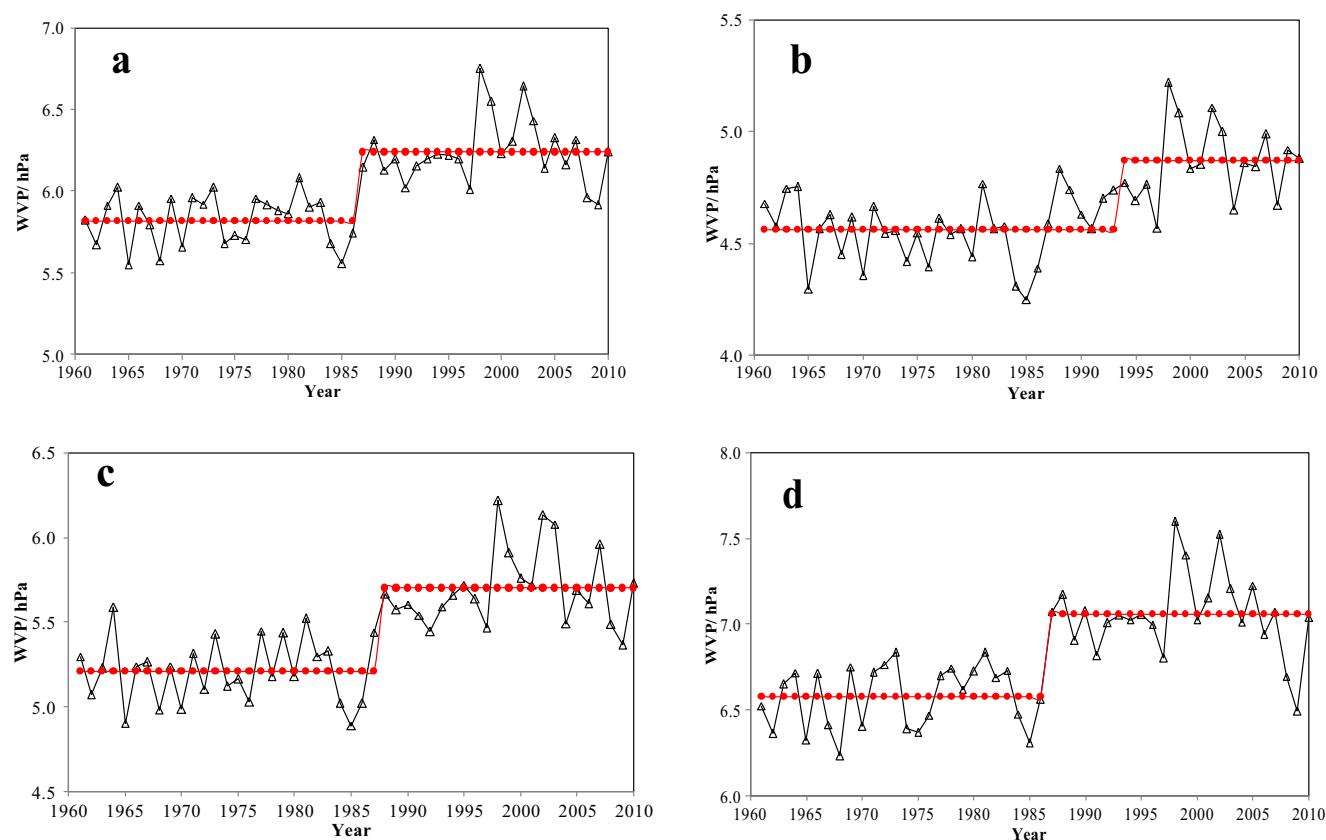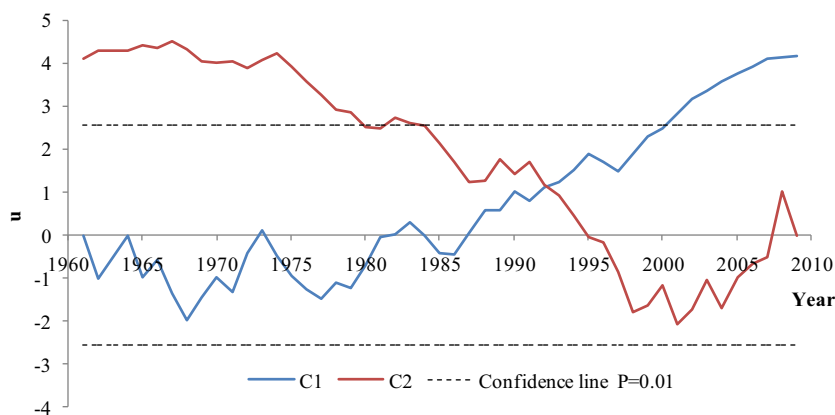

Fig. 6 Abrupt change of water vapor in the entire region (**a**), mountain (**b**), desert (**c**), and oasis (**d**) landscapes

Fig. 7 The abrupt change tested by the Mann–Kendall method for WVP in Bole station from 1961 to 2011. In here, as the line C1 is over the confidence line ($P=0.01$), the cross point of C1 and C2 is the start point of abrupt change in this series

precipitation (Chen and Xu 2005; Zhang et al. 2010; Li et al. 2012a). Figure 6 shows that the abrupt change point in the AMWVP of oasis occurred in 1986, followed by the desert in 1987, and the mountain in 1993, which are related to the unique geographical position and climatic conditions in different landscapes. Since the abrupt change analysis reveals that the entire and three landscapes had relatively abrupt changes around 1990, we divided the 51 years into two periods, before and after 1990, and conducted more detailed analysis to each. As shown in Fig. 6, the AMWVC in the second period is markedly higher in all landscapes.

Compared with the period 1961–1989, the AMWVP during the period 1990–2011 in the desert landscape increased the largest, increasing by 0.49 hPa, followed by those in the oasis landscape, increasing by 0.48 hPa, while those in the mountain landscape increased the smallest, increased by 0.31 hPa. In general, the AMWVP in the desert landscape increased most rapidly, followed by that in the oasis landscape, and the lowest one is in the mountain landscape. The reasons for these mainly lie in two aspects. One reason is that the ecosystem in the desert area has low stability and the mountain ecosystem has high stability; the other reason is that the ARNC has experienced a rapid population growth, along with fast expansion of urbanization, industrialization, and tourism since 1990. Human interference activity effect may cause the

difference among different landscapes under the background of global warming and regional climate change.

3.4 Abrupt change of WVP

The M-K abrupt change method with a nominal rejection rate of 1 % was applied to 96 stations of the WVP series. The Bole station (82.07° E, 44.9° N) was selected as an example to demonstrate the abrupt change happening in the time series of WVP. It showed that the abrupt change occurred in 1992 (Fig. 7). By this method, the abrupt changes were detected for 96 time series of WVP in the ARNC, and significant trends for different stations are shown in Fig. 8. Only 17 among 96 stations showed no significant trend, and the remaining 79 stations exhibited a significant trend ($P=0.01$, and $P=0.05$ for five stations). Among the 79 stations with significant trend, four stations (Edina, Zhongwei, Yongchang, and Guizihu) showed a downward trend and 75 stations displayed an upward trend. The distribution of the trend for the WVP revealed that no trend and downward trend abrupt changes were mainly in the northwest of the Ningxia Autonomous Region, western of the Inner Mongolia Autonomous Region, and southeast of the Hexi Corridor and water vapor in these area had no significant change. Adversely, in the northwest and middle portion of the Xinjiang Autonomous Region and northwest of the

Fig. 8 The upward trends (*blue*), downward trends (*red*), and no trends (*gray*) in the WVP during 1961–2011 detected by the Mann–Kendall method in the ARNC
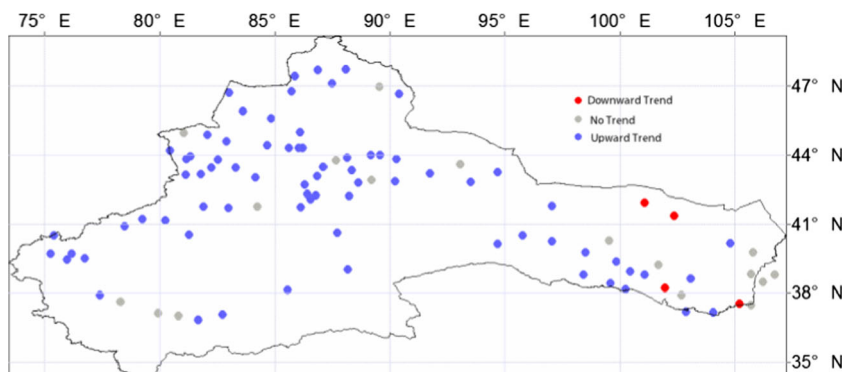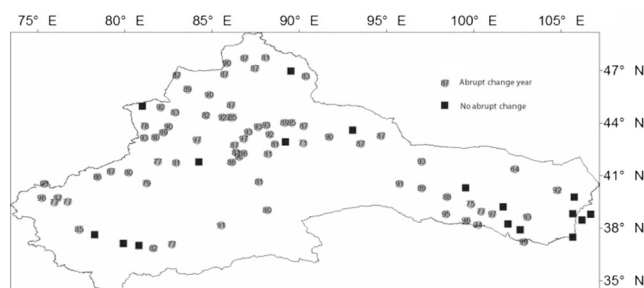
Fig. 9 The year of the abrupt change detected by the Mann–Kendall method in the meteorological stations of ARNC; the year when the abrupt change happened has been simplified in two figures, e.g., 87 for 1987

Hexi Corridor, the upward trend abrupt change had been presented in most of the stations.

The year of the abrupt changes tested by the M-K method is shown in Fig. 9. The results indicated that the abrupt change ranged from 1964 to 1999 in the recent 50 years. Two or three abrupt changes are detected in the following seven stations: Khorgos, Xinyuan, Yining, Ejina, Dunhuang, Zhongwei, and Jingtai; these stations are located in the northwest of Xinjiang and northwest of the Hexi Corridor, which indicated that this region was sensitive to the climate change. Furthermore, there were 35 abrupt changes happened from 1981 to 1990, 22 ones from 1991 to 1999, 12 ones from 1971 to 1980, and only 1 from 1961 to 1970. Especially, 11 abrupt changes happened in 1987, 8 ones happened in 1993. In this abrupt change year, vegetation cover has changed considerably due to the climate change and human activities. In the northwest Xinjiang, the change of vegetation cover has changed considerably due to the climate transited from warm dry to warm wet in the 1987 (Fang et al. 2013; Shi et al. 2007). In the Hexi Corridor area, the vegetation cover also improved because of better water supply and management (Ma et al. 2003). The reasons for the abrupt change of the WVP in the ARNC are needed to further study the interaction between the climate change, land use/land cover, and human activities.

4 Conclusions

In this paper, the M-K nonparametric trend and abrupt change test were used to reveal the spatial and temporal variability of WVP in the arid region northwest of China during 1960–2010. The results presented as follows:

1. The WVP possesses vertical zonality and longitude zonality, which decreased from the low to high with the elevation increasing, and the WVP changed obviously from the northwest and southeast to the middle of the ARNC. Among the different landscapes, the WVP high values are found in oasis area and the low values in mountainous and desert areas. In the mountainous area, the

WVP of Qilian mountains is greater than that of Tianshan mountains in the same height. The larger-scale atmospheric circulation, geographical situation, and elevation composed a complex condition to influence the spatial distribution of AMWVC in ARNC.

2. The results indicated that the WVP has significant increasing trends for the period 1961–2011 ($P<0.01$) and the abrupt change points in 1986 ($P<0.001$). Among the three landscapes, the WVP in the desert increased most rapidly, followed by that in the oases, and the lowest one is in the mountains.

3. The results of M-K analysis exhibited that 79 stations experienced abrupt WVP change, 75 with upward trends and 4 with downward trends, and the other 17 stations have no abrupt change during the recent 51 years, however. For the abrupt change year, 11 abrupt changes happened in 1987 and 8 ones happened in 1993.

4. The northwest of Xinjiang and northwest of the Hexi Corridor were sensitive to the water vapor change, because the most of abrupt changes occurred here during the period of 1961–2011. In this region, the land cover has been changed a lot owing to the human activity, so further studies should be performed on the relations between the land use and cover and the water vapor change.

References

Abbott PF, Tabony RC (1985) The estimation of humidity parameters. Meteor Mag 114:49–56

Bengtsson L (1997) The numerical simulation of climatic change. Ambio 26:58–65

Brohan P, Kennedy JJ, Harris I, Tett SFB, Jones PD (2006) Uncertainty estimates in regional and global observed temperature changes: a new data set from 1850. J Geophys Res 111, D12106. doi:10.1029/2005JD006548

Canada E (1977) Manual of surface weather observations. Atmos Environ Serv 440

Chen YN (2014) Water resources research in the arid region of northwest China. Chinese Science Press, China (in Chinese)

Chen YN, Xu ZX (2005) Plausible impact of global climate change on water resources in the Tarim River Basin. Sc China Ser D Earth Sci 48:65–73

Dai XG, Wang P (2010) Zonal mean mode of global warming over the Past 50 Years. Atmospherie and oceanic science Letters 3(1):45–50

Fang SF, Yan JW, Che ML et al (2013) Climate change and the ecological responses in Xinjiang, China: model simulations and data analyses. Quat Int 311:108–116

Fu CB, Wang Q (1992) The definition and detection of the abrupt climatic change. Scientia Atmos Sinica 16(4):482–493 (In Chinese)

Held IM, Soden BJ (2000) Water vapor feedback and global warming. Annu Rev Energy Environ 2525(2):445–475

Hu RJ, Jiang FQ, Wang YJ et al (2002) A study on signals and effects of climatic pattern change from warm-dry to warm-wet in Xinjiang. Arid Land Geography 25(3):194–200

Huang RH, Zhang ZZ, Huang G (1998) Characteristics of the water vapor transport in East Asian monsoon region and its difference from that in south Asian monsoon region in summer. Chin J Atmos Sci 22(4): 460–469

IPCC (2007) Climate Change 2007: The Physical Science Basis. Contribution of Working Group I to the Fourth Assessment Report of the Intergovernmental Panel on Climate Change, edited by S. Solomon et al., Cambridge Univ. Press, Cambridge, U. K.

Jin LY, Fu JL, Chen FH (2006) Spatial and temporal distribution of water vapor and its relationship with precipitation over Northwest China. J Lanzhou University (Natural Sciences) 42(1):1–6 (in Chinese)

Kahya E, Kalayci S (2004) Trend analysis of streamflow in Turkey. J Hydrol 289:128–144

Kendall MG (1948) Rank correlation methods. Hafner, New York

Li B, Chen Y, Shi X et al. (2012) Temperature and precipitation changes in different environments in the arid region of northwest China. Theor Appl Climatol doi:10.1007/s00704-012- 0753–4

Li, B, Chen Y, and Shi X (2012) Why does the temperature rise faster in the arid region of northwest China? J. Geophys. Res., 117, D16115, doi: 10.1029 /2012JD 017953.

Liu Q, Yang ZF et al (2008) Spatial and temporal variability of annual precipitation during 1961–2006 in Yellow River Basin, China. J Hydrol 361:330–338

Ma M, Dong L, Wang X (2003) Study on the dynamically monitoring and simulating the vegetation cover in Northwest China in the past 21 years. J Glaciol Geocryol 25:232–236 (in Chinese)

Mann HB (1945) Non-parametric test against trend. Econometrika 13: 245–259

Ren GY, Xu MZ, Chu ZY, Guo J, Li QX, Liu XN, Wang Y (2005) Changes of surface air temperature in China during 1951–2004. Clim Environ Res 10(4):717–727 (in Chinese)

Shi YF, Shen YP, Kang E, Li DL, Ding YJ, Zhang GW, Hu RJ (2007) Recent and future climate change in northwest China. Clim Chang 80(3–4):379–393. doi:10.1007/s10584-006-9121-7

Sun HL, Chen YN, Li WH et al (2010) Variation and abrupt change of climate in Ili River Basin, Xinjiang. J Geogr Sci 20(5):652–666. doi: 10.1007/s11442-010-0802-9

Wang JW (1995) Oasis, oasis making and oasis construction. J Arid Land Resour Environ 9(3):1–11 (In Chinese)

Wang XR, Xu XD, Miao QJ (2003) Regional characteristics of summer precipitation and water vapor amount in Northwest China. Climatic Environ Res 8(1):35–42

Wang YR, Lin SL, Yao H, Dong AX (2006) Response of atmospheric vapor over Gansu province to global climate change. Arid Land Geography 29(1):47–52 (In Chinese)

Wei N, Gong YF, Sun X, Fang JG (2010) Variation of precipitation and water vapor transport over the Northwest China from 1959 to 2005. J Desert Res 30(6):1450–1457 (In Chinese)

Wentz F, Ricciardulli L, Hilburn K, Mears C (2007) How much more rain will global warming bring? Science Express 317:233–235

Wu YP, Shen YP, Li BL (2012) Possible physical mechanism of water vapor transport over Tarim River Basin. Ecol Complex 9:63–70

Yao JQ, Yang Q, Hu WF et al (2012) Characteristics analysis of water vapor contents around Tianshan Mountain area and the relationships with climate factors. Sci Geogr Sin 33(7):859–864 (In Chinese)

Zhang Q, Zhang CJ, Bai HX, Lin L et al (2010) New development of climate change in northwest China and its impact on arid environment. J Arid Meteorol 28(1):1–7 (In Chinese)

Zhao RX, Wu GX, Zhang H (2008) Seasonal characteristic and interannual variability of the atmospheric hydrological cycle in the Yangtze River basin during the summer monsoon period. Chin J Geophys 51(6):1670–1681

Zhou TJ, Yu RC (2005) Atmospheric water vapor transport associated with typical anomalous summer rainfall patterns in China. J Geophys Res 110:D08104.1–D08104. 10